

Universal Velocity Profile Measurement of a Turbulent Channel Flow with a Fiber-Optic Velocity-Profile-Sensor

K. Shirai, L. Büttner, T. Pfister, J. Czarske (TU Dresden),
H. Müller, D. Dopheide (PTB),
S. Becker, H. Lienhart, F. Durst (LSTM)

Technische Universität Dresden (TU Dresden),
Helmholtzstraße 18, D-01069 Dresden
Email: czarske@iee.et.tu-dresden.de, Internet: www.lasermetrology.de

Physikalisch-Technische Bundesanstalt (PTB), Fachbereich 1.4 Gase
Bundesallee 100, D-38116 Braunschweig

Friedrich-Alexander-Universität Erlangen-Nürnberg, Lehrstuhl für Strömungsmechanik (LSTM)
Cauerstraße 4, D-91058 Erlangen

Abstract

The universal velocity profile in turbulent boundary layers was measured with a new fiber-optic velocity-profile-sensor. The sensor was realized with a frequency-division-multiplexing technique for high spatially resolved velocity measurements in turbulent boundary layers. As it has a spatial resolution inside the measurement volume, velocity measurement with a high spatial resolution is possible compared to the measurements with conventional laser Doppler anemometry. The new sensor has a capability of measuring the velocity close to zero, which is suitable for the near-wall measurements. The measurement accuracy of the sensor was experimentally investigated. The sensor successfully resolved the velocity profile in laminar boundary layers close to the wall. Then universal velocity profile in turbulent boundary layer was obtained in a fully developed turbulent flow. It is the first report on the application of the velocity-profile sensor to measure the universal velocity profile in turbulent boundary layers.

1. Introduction

Velocity information in the near-wall region of a high Reynolds-number flow is important for fundamental research and industrial applications of fluid mechanics. Recent developments of numerical simulations have enabled detailed analysis of a flow with relatively simple configuration. However, such simulations are still limited to flows with moderate Reynolds numbers (Moin and Mahesh 1998). On the other hand, many measurement methods have been developed through experimental investigations. Among them hot-wire anemometry (HWA) and laser Doppler anemometries (LDA) are two major techniques used for the measurements in turbulent flows, because of their relatively high spatial and temporal resolution compared to other methods. As the spatial resolution is determined by the size of the measurement volume, sensors cannot resolve flow phenomena with smaller scale than the size of the measurement volume. The information of such small scale motion is spatially averaged. When flow Reynolds number increases, the smallest scale of the flow becomes smaller and sensors suffer from the spatial averaging effect. Therefore, velocity measurement in the near-wall region of a high Reynolds number flow is still one of the challenging works in fluid mechanics.

A velocity-profile sensor was proposed in order to avoid the longitudinal spatial averaging effect of LDA (Czarske 2001). It utilizes two fringe systems for a measurement volume and enables velocity measurement with a spatial resolution inside the measurement volume. Hence, higher spatial resolution can be achieved compared to that of a conventional LDA. Recently a spatial resolution in sub-micrometers range was achieved (Büttner and Czarske 2005). In former works, the velocity-profile sensors had been successfully applied to laminar boundary layers (Czarske et al., 2002). However, their application to the region, where the flow velocity becomes close to zero, was not possible because the evaluation of Doppler frequencies was done in the base-band. The use of a high pass filter hindered the sensor from distinguishing the Doppler-frequency peak corresponding to zero velocity from the contribution by the pedestal part.

In the present work we report about the development of a new velocity-profile sensor and its application to the measurement of the universal velocity profile in turbulent boundary layers. The new heterodyne velocity-profile-sensor was realized with only one wavelength of laser and with a frequency-division-multiplexing (FDM) technique, which enables the measurements close to the wall. A commercial fiber-optic LDA measurement head was used for flexible applications of the sensor. The developed sensor was first tested in laminar boundary layers and then applied to turbulent boundary layers in a fully developed channel flow. An adaptive signal processing technique was developed and applied for the sensor to evaluate the measurement signals in turbulent boundary layers, which is described in details in Shirai et al. (2005).

2. Fiber-Optic Velocity-Profile-Sensor

The basic principle of the velocity-profile sensor is the use of two interference-fringe systems in the measurement volume. The details of the principle are described in Czarske (2001) and Czarske et al. (2002). The sensor resolves the position of a tracer particle along the optical axis as well as the velocity of a particle passing through the measurement volume. Therefore, high spatially resolved velocity measurement of a flow is possible.

Setups of Sensor

Fig. 1 shows the setup of the FDM profile-sensor. The beam from a laser (wavelength: 532 nm) was split into two partial beams using a beam splitter cube. Subsequently, the beams were further divided into two beams by acousto-optic modulators (AOMs), which were operated with a frequency shift of 120 MHz and 60 MHz, respectively. Only the beams of the 0th and the +1st diffraction order of the AOMs were allowed to pass and all the other beams were blocked. The 0th order beam split by the AOM with 60 MHz was led through another AOM with 80 MHz frequency shift. Each of the resulting four partial beams, which experienced different frequency shifts of 120 MHz, 0 MHz, 80 MHz and 60 MHz respectively, was coupled into a single-mode fiber (SMF) and guided toward a commercial two-component LDA-measurement-head. The optical fibers were connected to the head so that two pairs of fringe systems with 120 MHz and 20 MHz were obtained (Fig. 2). The combinations of the beams were carefully chosen in a way that none of other pairs of difference frequencies between two individual beams coincides with the two carrier frequencies of 120 MHz and 20 MHz. Remaining parasitic frequencies in Doppler signals were eliminated by low-pass filters so that they don't influence the measured signals.

The measurement volume was formed at the intersectional area of beams, which was about 300 mm apart from the measurement head. Because of the arrangement of the beams at the head, the two fringe systems were tilted about 3.6 degrees with respect to the optical axis

(Fig. 3). As a result, the effective length of the measurement volume was smaller than that of the individual fringe system.

Fig. 3 shows the setup of the detection part. The scattered light from a tracer particle passing through the measurement volume was coupled into a multi-mode fiber (MMF) and guided into a photo detector. The electrical output from the detector was split into two channels. The signal of each channel was mixed down into the baseband with each carrier frequency of 120 MHz and 20 MHz, which were created by using the reference outputs of the AOM drivers. The 20 MHz reference signal was generated by mixing the 60 MHz and 80 MHz driver signals and by applying a band-pass filter with a central frequency of 20 MHz. Then low-pass filters were applied to the down mixed signals to suppress the parasitic signals. A major advantage of the setup was the robustness to drifts in the AOM driver frequencies. Even if the driving frequency changed, it did not give any serious influence on the measurement since the same oscillators were used for frequency shifting and down mixing. Thus a complex circuitry was not necessary for frequency stabilization. The down mixing enabled measurement close to zero velocity since no DC-pedestal occurred in the power spectra. Measurement data were acquired with a two-channel 12-bit A/D converter card built in a standard PC. The signals from the both channels were acquired simultaneously and a LabVIEW program controlled the measurements.

After the data acquisition further signal processing was realized in software. Two different methods were used: one was online processing during the measurement and the other was offline processing. The online method evaluated the position and velocity information with validation steps. The offline method was applied mainly for the measurements in turbulent boundary layers. Triggered signals were stored as raw time signals without any processing during the measurements. They were processed afterwards with specially developed software after the measurement. The software detected signal part in the raw data and processed each of them with validation steps. This was necessary to detect signals with a wide range of velocity in the measurement volume especially for the measurements close to the wall. The details of these processing techniques are described in Shirai et al. (2005).

Measurement Accuracy

First the beams at the sensor head were adjusted to create the measurement volume. They were adjusted so that they cross at one point and create two fringe systems with respective fringe spacing diverging and converging along the direction of optical axis. Then the sensor was calibrated with a thin metal wire. The wire was served as a scattering object and it was attached on the wheel of an optical chopper, which rotated at a stabilized angular speed. The chopper was mounted on a motorized translation table and scanned through the measurement volume along the optical axis. The fringe spacings of the corresponding channels, $d_1(z)$ and $d_2(z)$, were calculated from the known constant velocity of the wire and the measured Doppler frequencies at each position z along the optical axis (Czarske et al. 2002). At each position several 10 samples were taken and averaged in order to reduce statistical uncertainty. Finally quotient curve $q(z) = d_1(z)/d_2(z)$ was determined from the measured Doppler frequencies as shown in Fig. 4. The actual size of the measurement volume was estimated to be about 900 μm from the frequency amplitude of the power spectra.

The measurement accuracy and the spatial resolution of velocity-profile sensor were estimated by the method based on Czarske et al. (2002). Relative velocity-measurement accuracy is mainly determined by the accuracy of Doppler-frequency estimation. The spatial resolution of the sensor depends on the accuracy of Doppler-frequency estimation and the slope of the calibration curve. From the calibration experiment the relative velocity-measurement accuracy was estimated to be 0.26 % and the spatial resolution was about 5 μm in the central region of the measurement volume.

3. Results and Discussions

Laminar boundary layer

The sensor was tested in a laminar boundary layer in a Göttingen-type wind tunnel. A glass plate was inserted in the uniform flow and forward-scatter detection was used for the signal detection. For tracer particles, diethyl-hexyl-sebacate (DEHS) was used with an atomizer. The measurement signals were processed online.

Fig. 5 shows the measurement result in a laminar boundary layer with a theoretical curve of Blasius solution. The velocity was normalized with the free-stream velocity U_∞ . A non-dimensional parameter was used for the horizontal axis (White, 1991)

$$\eta = z \sqrt{\frac{U_\infty}{2\nu x}}, \quad (1)$$

where ν is the kinematic viscosity of the fluid and x is the distance from the leading edge to the measurement point. The plot consists of about 2500 individual data points measured in the flow. The velocity profile was successfully reproduced despite the fact that no averaging or smoothing was used for the plot. The reproduced profile agrees well with the Blasius profile. For obtaining the profile the measurement head was traversed 10 times because of the thickness of the boundary layer. Due to the down mixing, the velocity measurement close to zero became possible. The smallest velocity measured was 0.03 m/s and this indicates the sensor has a potential to be applied to flow measurements close to the wall in turbulent boundary layers.

Turbulent boundary layer

The FDM sensor was applied to turbulent boundary layers in a fully developed two-dimensional air channel flow. The dimensions of the cross-section were 600 mm x 50 mm, which ensured the two dimensionality of the flow (Dean, 1978). The flow was tripped at the entrance of the channel to enhance the transition to turbulence. The details of the flow apparatus are described in Zanoun et al. (2003). The measurement was conducted at about 6000 mm from the inlet, which corresponds to 120 H (H : full channel height of wall to wall). This length was considered to be sufficient to obtain a fully developed condition of turbulent flow. At the measurement point a glass plate was attached to obtain an optical access for the measurement in forward scatter detection. The plate was mounted flush to the channel wall so that no flow disturbance occurs by inserting the plate. DEHS was used for tracer particles and the method of the offline signal processing was used for the measurements. The measurements were conducted with different conditions of Reynolds numbers. We define the Reynolds number as

$$\text{Re}_B = \frac{U_B H}{\nu}, \quad (2)$$

where the U_B denotes the bulk mean velocity, and it was independently measured by the manometer reading of pressure near the inlet of the flow.

Fig. 6 shows the measured mean velocity-profile of the channel flow at $\text{Re}_B = 4 \times 10^4$. The sensor head was traversed 34 times to obtain this profile and a total number of 30024 points were validated after the signal processing out of 67125 stored data. More numbers of data were acquired in the region close to the wall compared those in the region apart from the wall.

In the plot every 200 data points in the neighborhood were averaged about their position and velocity in order to reduce the scattering of data points. This means that each point represents the average of 200 points with respect to both the position and the velocity. Each individual data point was used only once for the average. This method was chosen for the effective use of the measured information about the position and velocity of each particle. There is a different method to calculate statistics by setting slots with constant width for the position and making average of each slot (Büttner et al. 2004). However, it doesn't give average with same statistical accuracy for all the slots due to the non-equally distanced and non-equal numbers of data distribution. The present result shows fairly good agreement with a direct numerical simulation (DNS) by Abe et al. (2001) although it shows deviation a little apart from the wall ($Z/(H/2)=0.03\sim 0.16$). This is perhaps due to the different Reynolds number of the flows and relatively small number of data points taken in the present measurement.

In Fig. 7 the normalized profiles of mean-velocity and fluctuating-velocity are shown. The flow Reynolds number was $Re_B = 1.8 \times 10^4$. The axes were normalized with friction velocity $u_\tau = \sqrt{\tau_w / \rho}$ (ρ : the fluid density). The wall shear stress τ_w is defined by

$$\tau_w = \mu \left. \frac{dU}{dz} \right|_{\text{wall}}, \quad (3)$$

(μ : viscosity) and it was determined by the linear fit of the measured velocity profile close to the wall. The statistics were calculated for every 400 points in the neighborhood with respect to the position and the velocity. The mean velocity profile is shown with the linear fit equation and the log-law fit equation:

$$U^+ = (1/\kappa) \ln z^+ + B. \quad (4)$$

The constants κ and B obtained by the fit were $\kappa=0.29$, $B=6.5$, which are different from the values $\kappa=0.41$, $B=5.5$ in general (Bernard and Wallace, 2002). This is due to the low accuracy of the linear fit close to the wall. The friction velocity obtained by the fit was lower than the value estimated with an empirical equation by Dean (1978). It originates from the relatively small number of data points taken in the present measurement and the existence of outlier points. The outlier points were caused by the particle stuck on the wall, which made lower estimate for the velocity gradient close to the wall. The use of side-scatter detection and a stable laser with higher optical power could reduce the number of outliers. The fluctuating velocity (Fig. 7 (b)) shows a similar trend that the fluctuation values are higher than the results generally reported by other experiments and simulations. It was also due to the low estimate of the friction velocity, which was used for the normalization. The position, where the fluctuation became a peak, is around $z^+ \sim 11$, which is lower than the position $z^+ \sim 15$ reported in general (Bernard and Wallace, 2002). The distribution shows large fluctuation and because of relatively small number of data points for calculating the statistics.

4. Conclusion

Universal velocity profile in turbulent boundary layers was measured with a new fiber-optic velocity-profile-sensor. It can resolve the position of a tracer particle passing through the measurement volume, and hence high spatially resolved velocity measurement is possible. The use of heterodyne and FDM techniques enabled velocity measurement close to the wall. Fiber optics realized more flexible and robust measurement compared with the former velocity-profile sensors. The sensor had a relative velocity measurement accuracy of 0.26 % with a spatial resolution of the sensor about 5 μm inside the measurement volume of about

900 μm . The working distance was a working distance of about 300 mm. The sensor was tested in a laminar boundary layer. It successfully resolved the velocity distribution close to the wall. Then the sensor was applied in turbulent boundary layers in a fully developed flow. The measured mean and fluctuating velocity showed fairly good agreement with a DNS result. However, there were discrepancies between the present results and others. They were considered due to relatively small numbers of data points in the present measurements and the low estimate of friction velocity caused by the outlier data points. These can be reduced by more numbers of measurement data and by using side-scatter detection together with the use of a stable laser source with high optical power.

References

- H. Abe, H. Kawamura and Y. Matsuo (2001) Direct numerical simulation of a fully developed turbulent channel flow with respect to Reynolds number dependence, *ASME J. Fluids Eng.*, vol. 123, pp. 382-393.
- P. S. Bernard and J. M. Wallace (2002) *Turbulent flow*, John Wiley and Sons.
- L. Büttner, T. Razik, J. Czarske, H. Müller, D. Doppeide, S. Becker, H. Lienhart, F. Durst (2003) Ortsaufgelöste Vermessung turbulenter Scherströmungen mittels Laser-Doppler-Profilsensor (in German), 11th GALA-Fachtagung: *Lasermethoden in der Strömungsmesstechnik*, pp. 1.1-1.8, September 9-11, 2003, Braunschweig, Germany.
- L. Büttner, J. Czarske, H. Knuppertz (2005) Laser-Doppler velocity profile sensor with submicrometer spatial resolution that employs fiber optics and a diffractive lens, *Appl. Opt.* vol. 44, pp. 2274-2280.
- J. Czarske (2001) Laser Doppler velocity profile sensor using a chromatic coding, *Meas. Sci. Technol.*, vol.12, pp.52-57.
- J. Czarske, L. Büttner, T. Razik, and H. Müller (2002) Boundary layer velocity measurements by a laser Doppler profile sensor with micrometre spatial resolution, *Meas. Sci. Technol.* vol.13, pp.1979-1989.
- R. B. Dean (1978) Reynolds number dependence of skin friction and other bulk flow variables in two-dimensional rectangular duct flow, *ASME J. Fluids Eng.*, vol. 100, pp. 215-223.
- P. Moin, K. Mahesh (1998) Direct numerical simulation: a tool in turbulence research, *Annu. Rev. Fluid Mech.*, vol. 30, pp.539-578.
- K. Shirai, T. Pfister, J. Czarske (2005) Signal Processing Technique for Boundary-Layer Measurements with a Laser-Doppler Velocity-Profile-Sensor, 13th GALA-Fachtagung: *Lasermethoden in der Strömungsmesstechnik*, pp. 4.1-4.8, September 6-8, 2005, Cottbus, Germany.
- F. M. White (1991) *Viscous fluid flow*. 2nd edition, McGraw Hill.
- E.-S. Zanoun, F. Durst and H. Nagib (2003) Evaluating the law of the wall in two-dimensional fully developed turbulent channel flows, *Phys. Fluids.*, vol. 15, pp. 3079-3089.

Figures

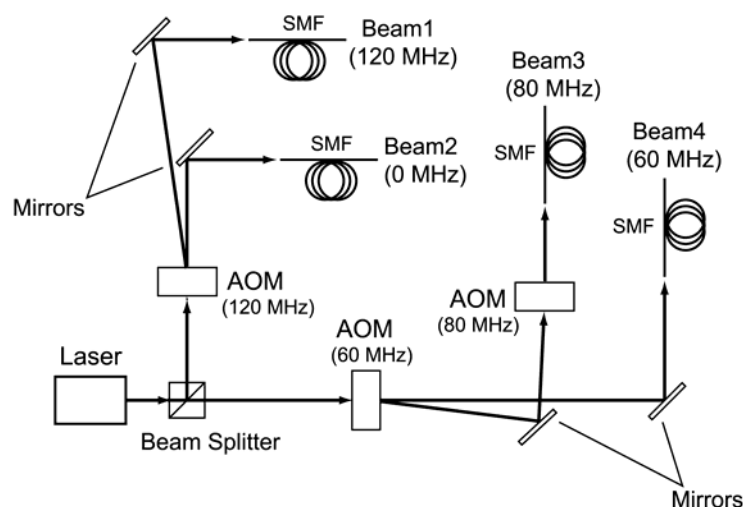


Fig. 1 Optical setup of the FDM velocity-profile sensor. (Three AOMs are used for shifting frequencies.)

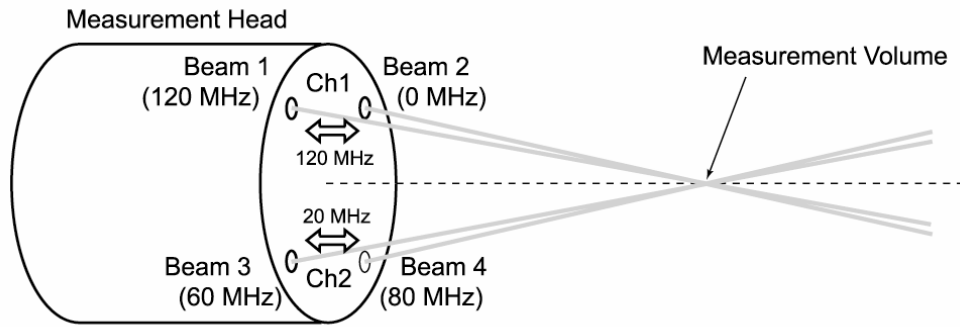


Fig. 2 The arrangement of the beams at the measurement head.

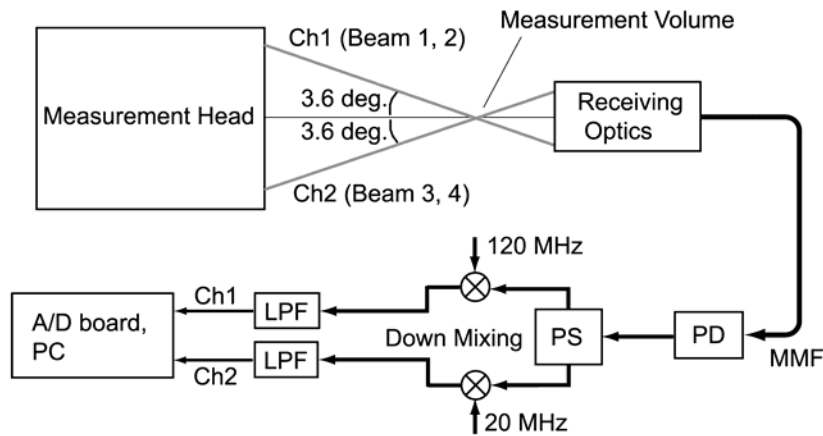


Fig. 3 Setup of the detection part of the FDM velocity-profile sensor. (MMF: multi-mode fiber, PD: photo detector, PS: power splitter, LPF: low-pass filter)

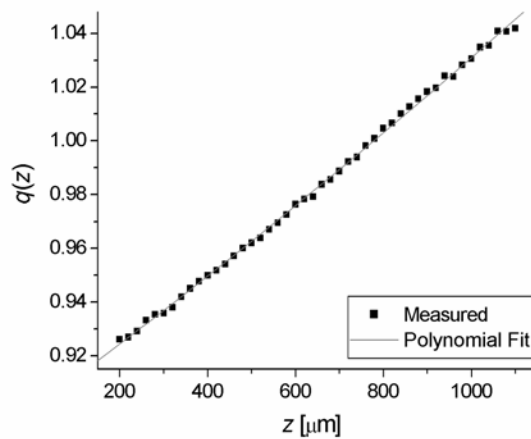


Fig. 4 Calibration function in the direction of the optical axis z used for the measurements in turbulent boundary layers.

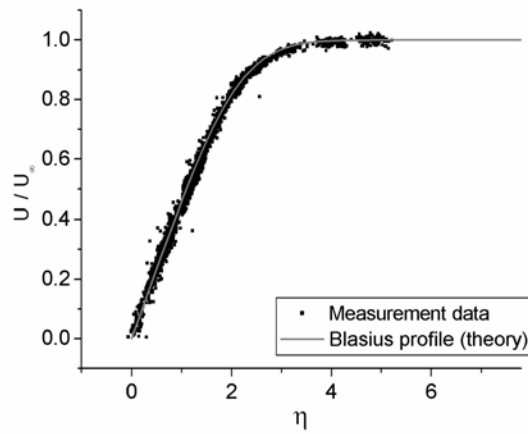


Fig. 5 Measured velocity profile in a laminar boundary layer compared with Blasius profile

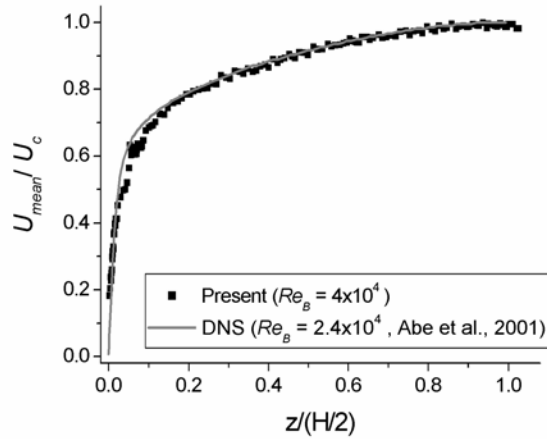


Fig. 6 Mean velocity-profile in measured in a turbulent channel flow. (Axes are normalized with channel-centerline velocity and half width.)

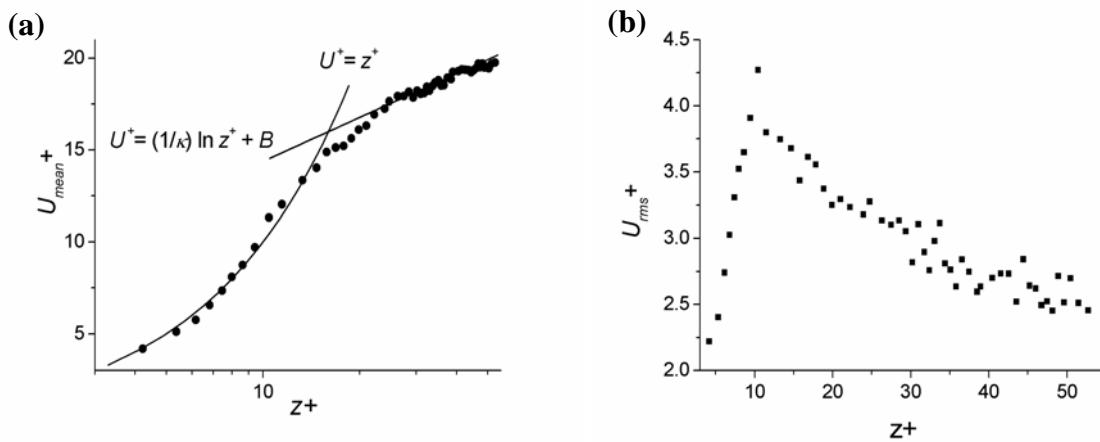


Fig. 7 Mean and fluctuating velocity near the wall: (a) mean velocity, (b) fluctuating velocity. (Values are normalized with wall variables.)